



INTERFACIAL WAVE SHAPE EQUATION IN HORIZONTAL WAVY STRATIFIED WATER-HEAVY OIL FLOW

Marcelo Souza de Castro

Oscar Mauricio Hernandez Rodriguez

Engineering School of Sao Carlos, University of Sao Paulo
Av. Trabalhador São Carlense, 400
13566-590, Sao Carlos, SP, Brazil
marscastro@gmail.com
oscarmhr@sc.usp.br

Abstract. *Liquid-liquid flows are present in a wide range of industrial processes; however, studies on such two-phase flow are not as common as those on gas-liquid flow. The interest in liquid-liquid flow has recently increased mainly due to the petroleum industry. Pressure drop, heat transfer, corrosion and structural vibration are a few examples of topics that depend on the geometrical configuration or flow patterns of the immiscible phases. The stratified flow pattern is commonly present in directional oil wells and pipelines. The interfacial wavy structure in gas-liquid flow has been studied by many authors and some findings were that this structure affects the friction factor and the heat transfer coefficients. On the other hand, studies on waves in stratified liquid-liquid flow are scanty. Regarding the interfacial wave shape in stratified liquid-liquid flow, there are almost no references. Therefore, the main goal of this work is to present a general equation based on Fourier Functions, where the coefficients are functions of dimensionless numbers, modified Weber and Froude numbers, for the interfacial wave shape in water-heavy oil flows. The findings are based on experimental data acquired at the Thermal-Fluid Engineering Laboratory of the Sao Carlos School of Engineering, USP.*

Keywords: *liquid-liquid flows, heavy oil-water flows, wavy stratified flow, interfacial wave, wave shape*

1. INTRODUCTION

Liquid-liquid flows are present in a wide range of industrial processes; however, studies on such two-phase flow are not as common as those on gas-liquid flow. The interest in liquid-liquid flow has recently increased mainly due to the petroleum industry, where oil and water are often transported together for long distances. Pressure drop, heat transfer, corrosion and structural vibration are a few examples of topics that depend on the geometrical configuration or flow patterns of the immiscible phases. The stratified and annular flow patterns are usually denominated separated flows. The stratified flow pattern is commonly present in directional oil wells and pipelines. This flow is characterized by the heavier and lighter phases located at the bottom and top part of the pipe, respectively, divided by an interface that can be smooth, wavy or present droplets of one phase into the other phase.

An experimental work on characterization of liquid-liquid flow patterns can be seen in Trallero (1995) and Trallero *et al.* (1997), where data for horizontal flow were presented including stratified and semi-stratified flow, dispersions and emulsions. Those authors did not differentiate wavy stratified from stratified with mixing at the interface. Elseth (2001) presented a more detailed horizontal oil-water flow pattern classification, dividing Trallero's patterns into several sub-patterns. Elseth (2001) observed the wavy stratified flow. Alkaya *et al.* (2000) continued the work of Trallero *et al.* (1997), but now introducing the effect of pipe inclination. A wavy stratified flow pattern was reported. All the quoted authors have dealt with relatively low viscosity oils. On the other hand, Bannwart *et al.* (2004) studied a horizontal very viscous oil-water flow and reported the stratified flow pattern among others. Interfacial waves in liquid-liquid stratified flow have been spotted, but details on the wave's geometrical properties were not given.

The interfacial wavy structure was studied in gas-liquid flow by Bontozoglou and Hanratty (1989) and Bontozoglou (1991). One of the findings was that the two-phase friction factor of wavy stratified flow can be about fifty times as high as the friction factor of smooth stratified flow. Li *et al.* (1997) also studied the gas-liquid stratified flow pattern and showed that the interfacial waves have significant influence on heat transfer and pressure drop. The interfacial wavy structure of separated flows in gas-liquid systems and its influence on the flow have been further studied by a few researches; the effect of interfacial waves on friction factor with or without gravity in annular flow, the role played by stratified-flow parameters on slug flow formation and a numerical solution for stratified flow that considers an effective roughness due to the waves have been the research subject of, respectively, Wang *et al.* (2004a and b), Dymant and Boudlal (2004) and Berthelsen and Ytrehus (2005). Brauner *et al.* (1996) compared the gas-liquid and liquid-liquid interfaces in stratified flow. In the former, a flat interface is more likely because the flow is dominated by gravitational forces, whereas the latter tends to present a curved interface since interfacial tension also plays a role.

The study of wave motion is a vast scientific topic; one can cite, for instance, ocean waves in deep or shallow waters. The study of interfacial wave behavior in two-phase flow is a relatively recent research topic, but of significant importance, since key parameters as holdup and pressure drop are expected to depend on the wavy structure. In

addition, an exponential increase in time or space of wave amplitude might cause instabilities and, eventually, flow pattern transition (Wallis 1969). There are a few studies in the literature on interfacial waves in core-annular flow. In Ooms (1972), Ooms *et al.* (1974) and Oliemans (1986) it was demonstrated that the existence of waves is fundamental for the stability of the core-annular flow pattern. Experimental data on the characteristics of the interfacial wave in the core-annular flow were presented by Bannwart (1998). Feng *et al.* (1995), working with numerical simulation, also found that waves are indispensable for the hydrodynamic stability of such liquid-liquid separated flow pattern. On the other hand, information on interfacial wave properties in liquid-liquid stratified flow is scanty, although it seems evident that it is crucial for the complete understanding of stratified flow. Some data are presented in Al-Wahaibi and Angeli (2007) and Al-Wahaibi *et al.* (2007), but it lacks of details on wave properties. Recently, Castro *et al.* (2012) used the data obtained by Pereira (2011) to make a preliminary analysis and showed that the oil-water interface properties are function of the relative velocity, holdup and pipe inclination angle.

As said, there are few works devoted to the systematic study of waves in stratified viscous oil-water pipe flow. So, the main goal of this work is to investigate the topological characteristic of the interfacial wave in the heavy oil-water stratified flow pattern, and propose a generic equation to predict the characteristics of these waves based on dimensionless numbers calculated with flow and fluid properties. This allows, for example, the simulation of the propagation of these waves in a pipeline. In Sections 2 and 3 the experimental setup and procedure are presented. The image processing technique used to measure wave properties is explained in Section 4. In Section 5 experimental data on aspect ratio, wave celerity and mean interfacial wave topology are offered. Section 6 presents the study on the generic wave to predict the properties and wave shape of the interfacial wave. Finally, the conclusions are drawn in section 7.

2. EXPERIMENTAL SETUP

The hydrophilic-oilphobic glass test line of 26-mm i.d. and 12-m length of the multiphase flow loop of the Thermal-Fluids Engineering Laboratory of the Engineering School of Sao Carlos at the University of Sao Paulo (LETeF) was used to observe different oil-water flow patterns. The test section has seven transparent boxes used to film the flow, in order to correct any remaining distortion of light due to lens and parallax effects, the boxes were filled with water. The first box is placed at 1.3 m from the beginning of the test line; the others are placed 1.5 m apart of each other. A schematic view of the flow loop and details related to the holdup measurement technique can be seen in Rodriguez *et al.* (2011). The water used in the experiments had density of 988 kg/m³ and viscosity of 1 mPa.s at temperature of 20 °C. The oil used had density of 828 kg/m³ and viscosity of 300 mPa.s at 20 °C. The viscosity was measured with a rheometer Brookfield™ model LVDV-III+ with rotor SC4-18. The oil-water interfacial tension was of 0,045 N/m. The oil-water contact angle with the borosilicate glass was 29° (hydrophilic-oilphobic). The interfacial tension and contact angle were measured with an optical tensiometer of KSV™ model CAM 200. The box placed at 4.3 m from the pipe entrance was used in the experiments presented in this paper.

3. EXPERIMENTAL PROCEDURE

The flow was recorded by a high-speed video camera (i-SPEED 3 OLYMPUS), which allowed the acquisition and optical measurement of the geometrical properties and celerity of the interfacial waves. The camera was installed on a pedestal. Two xenon lamps were used to illuminate the flow. The oil and water flow rates would be set and after reaching steady state the flow was recorded at a rate of 100 fps (frames per second) for 48 seconds at a resolution of 800x600 pixels. According to Pereira (2011) 30 fps would be enough to acquire all the information of the interfacial wave. A homemade LabView™-based program was used to extract the properties of the waves from the images (frames). The real-length-to-pixel conversion was done using the technique proposed by Pereira (2011). The experiments were carried out with the pipeline in the horizontal position. The inclination was measured using a BOSCH™ inclination meter model DN-ML 60 with accuracy of 0.1°. The water superficial velocity (U_{ws}) varied from 0.05 to 0.16 m/s, and the oil superficial velocity (U_{os}) varied from 0.02 to 0.18 m/s.

During the experiments it was observed that the wave properties seemed to be a function of the relative velocity and holdup. Therefore, two modified dimensionless number were proposed to correlate the experimental data of the interfacial wave. A modified Froude number (Fr^*), Eq. (1), correlates the wave celerity and a modified Weber number (We^*), Eq. (2), correlates the aspect ratio (ratio between wavelength and wave amplitude). Both the dimensionless number are function of a characteristic dimension defined in Eq. (3).

$$Fr^* = \frac{V_w - V_o}{\sqrt{g(\cos\theta)y_{car}}} \quad (1)$$

$$We^* = \frac{\Delta\rho(V_w - V_o)^2 y_{car}}{\sigma} \quad (2)$$

$$y_{car} = \varepsilon_w \frac{\pi D}{4} \quad (3)$$

In these equations $V_w - V_o$ is the relative velocity, θ is the inclination angle from horizontal, ε_w the water *in-situ* volumetric fraction, g the gravitational acceleration, D the pipe's internal diameter and $\Delta\rho$ is the difference between the densities of the fluids, and σ is the interfacial tension.

4. DATA TREATMENT

4.1 Interfacial wave properties

The Labview™ based software was used to identify the wave corresponding to the oil-water interface and predict its amplitude (α), wavelength (λ) and celerity (c). Each frame of the film is binarized (Fig. 1), bubbles and other noises are taken off the images. After those steps the interface is captured via a color contrast technique.

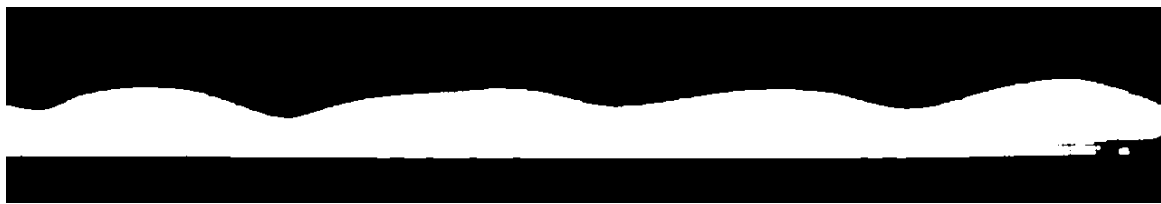


Figure 1. Binarized interfacial wave picture ($U_{ws}=0,09$ m/s and $U_{os}=0,1$ m/s).

All the peaks and valleys of the interface were found, and the waves of each image were separated. After finding the peaks and the valley of a wave, the algorithm fits a parabola between these points. It identifies and takes into account only the waves that have more than a predetermined quantity of points. Hence, ripples waves are eliminated. It was necessary to avoid interferences of the filter in the wave topology.

For each wave separated from the initial captured interface, the wavelength and wave amplitude are calculated using the definition of wave crest as the pixel in the spatial domain where the first derivative is zero, the next pixel has derivative lower than zero and the previous pixel has derivative greater than zero. The wavelength is the length difference between the abscissas (x -coordinate) of two followed crests. Since the interfacial wave is asymmetric, the definition of amplitude is not quite simple. It differs whether it is measured from the crest to the right or left valley (minimum value in the y -coordinate). To avoid this ambiguity, this paper uses the mean between the two calculated amplitudes (from the crest to the right valley and from the crest to the left valley) as the definition of wave amplitude. The celerity is calculated using cross-correlation between two frames lagged in time (Bendat and Piersol 2000). More details were presented by Castro et al. (2012).

4.2 Average wave shape

The methodology used to obtain the average topology of the wave was proposed by Castro et al. (2012). In the methodology proposed all the found waves were normalized, in each i -wave the x -coordinate is normalized by its wavelength and the y -coordinate is normalized by the pipe's internal diameter, *i.e.*, the dimensionless x^* - coordinate and y_i^* - coordinate are defined by Eqs. (4) and (5):

$$x^* = \frac{(x_i - x_{i,\min})}{(x_{i,\max} - x_{i,\min})} \quad (4)$$

$$y_i^* = \frac{y_i}{D} \quad (5)$$

As every i -wave has different dimensionless y_i^* - coordinates, Eq. (6) is applied in order to calculate the average dimensionless y^* - coordinate:

$$y^* = \frac{1}{k} \sum_{i=1}^k y_i^* \Big|_{x^*} \quad (6)$$

where k is the number of waves used for the purpose of wave shape determination. Finally, the average wave shape is given by the x_m - coordinate and y_m - coordinate:

$$x_m = \lambda_m \cdot x^* \quad (7)$$

$$y_m = D \cdot y^* \quad (8)$$

where λ_m is the mean wavelength between all the waves observed in a movie of each flow.

5. INTERFACIAL WAVE PROPERTIES

5.1 Wavelength, wave amplitude and celerity

The interfacial wave properties are functions of the dimensionless numbers given in Section 3; it was presented by Castro and Rodriguez (2013). Data of the ratio between wave celerity and mixture velocity are presented as function of the modified Froude number (Fig. 2a), presenting an exponential correlation (Eq. 9).

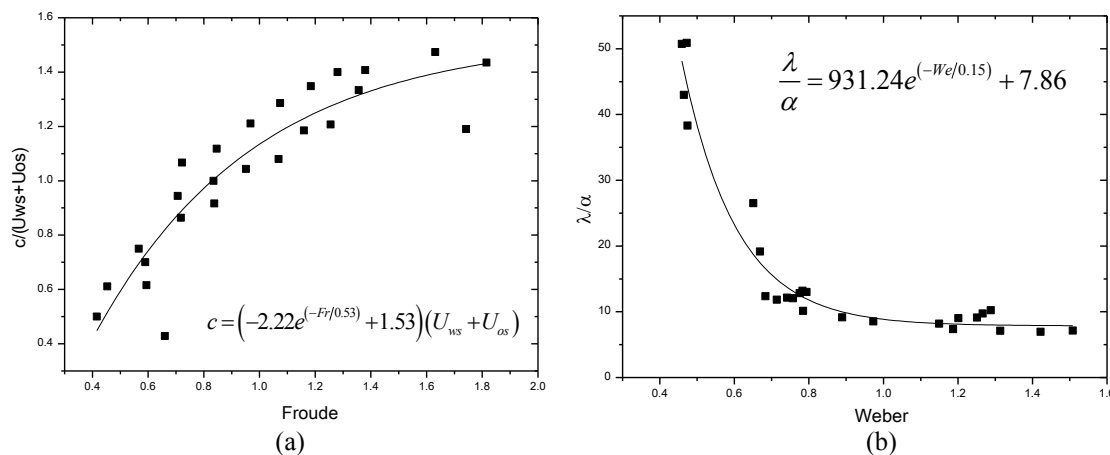


Figure 2. (a) Wave celerity as a function of the Froude number; (b) Wave aspect ratio as a function of the Weber number (Castro and Rodriguez, 2013).

$$c = \left[-2.22e^{(-Fr^*/0.53)} + 1.53 \right] (U_{ws} + U_{os}) \quad (9)$$

The aspect ratio of the interfacial wave of the heavy oil-water stratified flow pattern were plotted against the modified Weber number (Fig. 2b), and it presented, also, an exponential correlation given by Eq. (10).

$$\frac{\lambda}{\alpha} = 931.24e^{(-We^*/0.15)} + 7.86 \quad (10)$$

These data might be used to, given the parameters of a flow, superficial velocities, pipe diameter, fluid properties, and using models to predict the volumetric fraction of each phase achieve the properties that the interfacial wave of the flow should have. But, although this, the wave shape or topology remains an unknown. To correctly determine all the characteristics of the interfacial wave of the stratified flow the wave shape is one of the most important data. With this parameter analyses from the influence, for example of the relative velocity between the phases might be studied. For the known of the authors, the first time that the interfacial wave topology were presented was in the paper from Castro et al. (2012), but in that paper, the authors just presented the data without proposing a mathematical correlation to achieve the wave topology. This article intends to fill this gap for horizontal flows including new data on interfacial wave topology.

5.2 Wave shape

The technique proposed in Section 4.2 was used to get the interfacial wave shape. As pointed by Castro et al. (2012) the characteristics of the wave varies with the relative velocity between the phases. For a fixed oil superficial velocity

the variation of the water superficial velocity implies an increase of the wave amplitude without a big change in the wavelength. This might be seen in Fig. 3a, where the wave shape of several mean interfacial wave topology is presented for a fixed oil superficial velocity of 0.1 m/s, and the water superficial velocity varying from 0.05 to 0.13 m/s. The wave amplitude increase from about 0.6 mm to 2.7 mm as the water superficial velocity increases. Also, one might see the difference in the derivative from the sides of the wave, reminding a sea wave in the region of break. The flow occurs from the right to the left. The increase in the relative velocity makes the flow more unstable, and a bigger wave. This increase of the wave has a limit where droplets begin to be torn from the crest of these waves; this explains this increase.

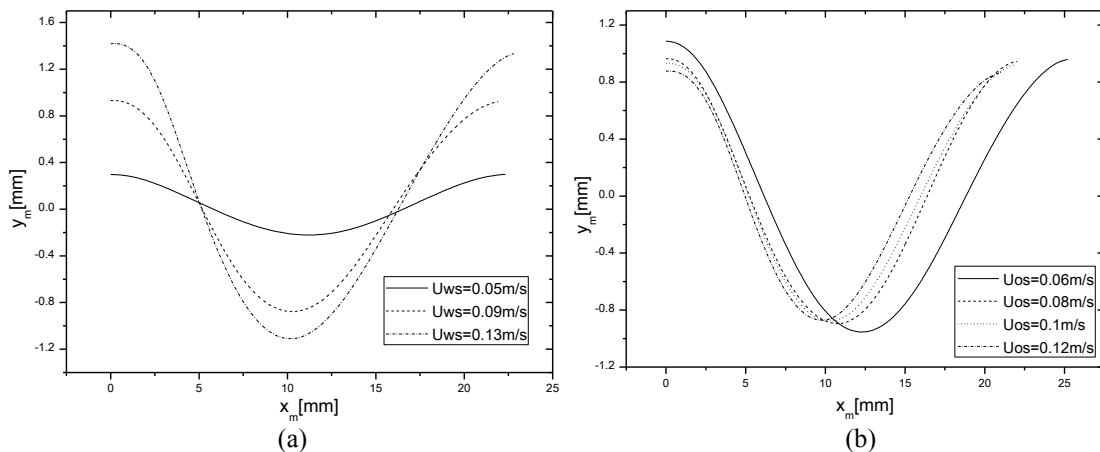


Figure 3. (a) Mean wave shape as function of the water superficial velocity for a fixed oil superficial velocity (0.1 m/s); (b) Mean wave shape as function of the oil superficial velocity for a fixed water superficial velocity (0.09 m/s).

In the case of fixing the water superficial velocity, and varying the oil superficial velocity, the wavelength varies, and the variation in the wave amplitude is marginal. As the oil superficial velocity increases the wavelength tends to decrease so the wave becomes narrower, so, more unstable, and the tendency of turning droplets from the interface is higher. Also, again there is the difference in the derivative from each side to the other of the mean interfacial wave, remembering the sea wave in the region of the break. These relations might be seen in Fig. 3b.

From the mean interfacial wave the wave of the flow might be rebuilt just making sequential waves of the same shape. The formed waves are compared with binarized images of the real flow at the same conditions. Examples of this reconstruction might be seen in Figs. 4 to 7. Figures 4 and 5 present the real and reconstructed interfacial wave for a flow with water and oil superficial velocities of 0.09 and 0.1 m/s, respectively. This wave has small amplitude and wavelength. Figures 7 and 8 present the real and rebuilt interfacial wave for in a flow with higher difference in the superficial velocities, so, a higher difference in the relative velocity. This flow has water and oil superficial velocities of 0.16 and 0.02 m/s, respectively. In this flow the wave amplitude is bigger, and also the wavelength. Looking at the Weber number of both flows, one might see that the on from the last flow is higher which propose a smaller aspect ratio of this wave instead of the first case.



Figure 4. Image of the real interfacial wave ($U_{ws}=0.09$ m/s and $U_{os}=0.1$ m/s).

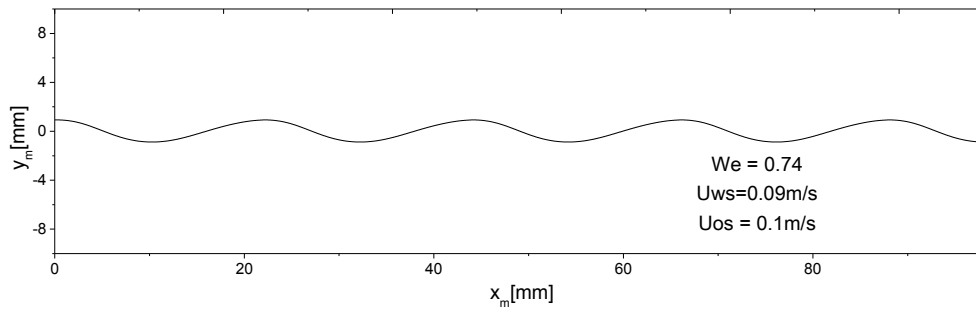


Figure 5. Mean interfacial wave rebuilt ($U_{ws}=0.09$ m/s and $U_{os}=0.1$ m/s).



Figure 6. Image of the real interfacial wave ($U_{ws}=0.16$ m/s and $U_{os}=0.02$ m/s).

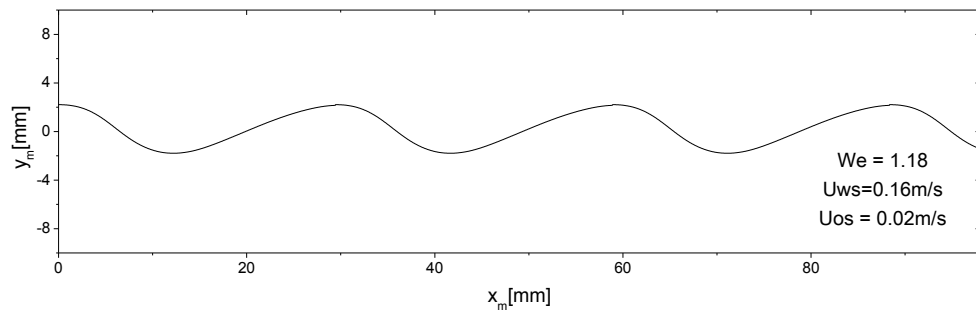


Figure 7. Mean interfacial wave rebuilt ($U_{ws}=0.16$ m/s and $U_{os}=0.02$ m/s).

All the conclusions made in this section were already published, but as said before, no references were observed about a mean mathematical function that describes this wave shape. This is the work that will be presented in the next section.

6. GENERIC INTERFACIAL WAVE EQUATION

6.1 Generic equation

The last section showed that the interfacial wave of the stratified oil-water flow might be rebuilt, and that this rebuilt is in good agreement with the experimental data. Now, a generic function that describes this wave is necessary, and will be made using a Fourier series of second order. Other orders were used, but higher orders only include more coefficients to be analyzed with almost no gain in the quality of the reconstruction. An equation with the form of Eq. (11) is proposed:

$$y_m = a_0 + a_1 \cos(wx_m) + b_1 \sin(wx_m) + a_2 \cos(2wx_m) + b_2 \sin(2wx_m) \quad (11)$$

The coefficients are a_0 to b_2 and w . The coordinates are x_m and y_m , given by Eqs. (7) and (8), respectively.

Using this series the mean waves were rebuilt and the result for one case in horizontal flow, with water and oil superficial velocities of 0.13 and 0.12 m/s, respectively, is showed in Fig. 8.

Using MatLab™ curve fitting tool, the coefficients (a_0 to w) for each mean wave were acquired. It was observed that these coefficients might be plotted against the proposed dimensionless numbers of Froude and Weber.

The a_0 coefficient was plotted against the modified Froude number, been well correlated by an exponential function (Fig. 9), given by Eq. (12).

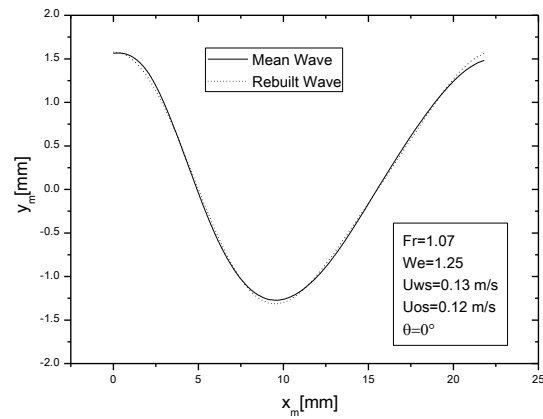


Figure 8. Comparison between mean wave and rebuilt by Fourier series ($U_{ws}=0.13\text{ m/s}$, $U_{os}=0.12\text{ m/s}$ and $\theta=0^\circ$).

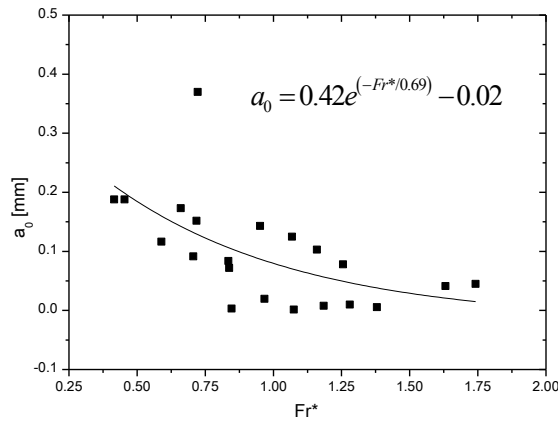


Figure 9. Coefficient a_0 as a function of the modified dimensionless Froude number.

$$a_0 = 0.42e^{(-Fr^*/0.69)} - 0.02 \tag{12}$$

Coefficient a_1 has a linear relation with Froude number, the experimental data is presented in Fig. 10. The equation that correlates the coefficient with the dimensionless parameter is given by Eq. (13).

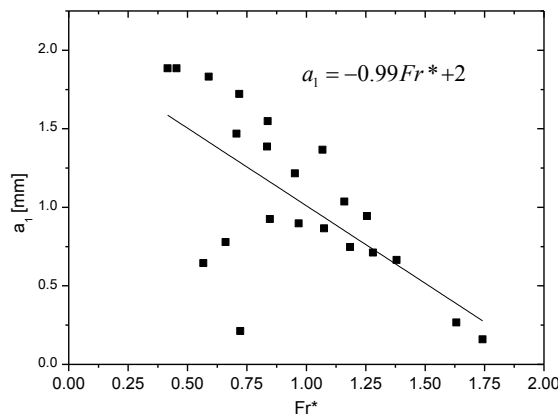


Figure 10. Coefficient a_1 as a function of the modified dimensionless Froude number.

$$a_1 = -0.99Fr^* + 2 \tag{13}$$

Coefficient a_2 is related to the modified dimensionless Weber number, also by a linear correlation. The graph is presented in Fig. 11, and the correlation is given by Eq. (14).

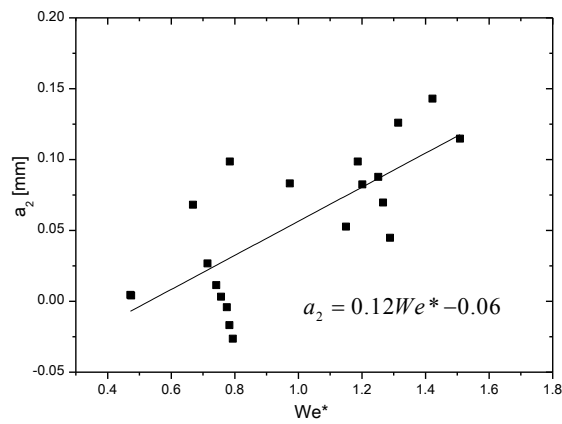


Figure 11. Coefficient a_2 as a function of the modified dimensionless Weber number.

$$a_2 = 0.12We^* - 0.06 \quad (14)$$

The coefficient b_1 is also linearly correlated by the modified Weber number, as coefficient a_2 . Figure 12 present the experimental data plotted against the proposed dimensionless number, and the linear correlation, given by Eq. (15).

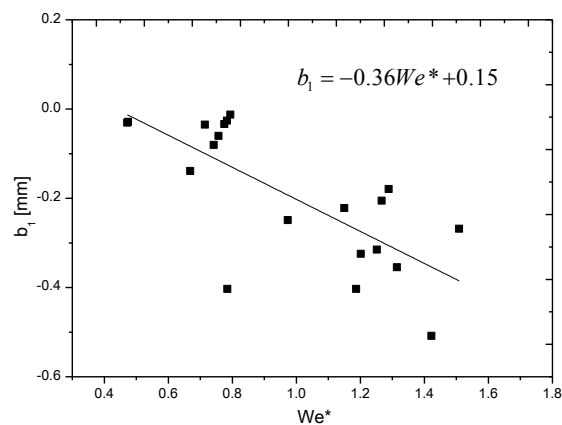


Figure 12. Coefficient b_1 as a function of the modified dimensionless Weber number.

$$b_1 = -0.36We^* + 0.15 \quad (15)$$

The last coefficients have, both, linear correlations with the Froude number. Experimental data on coefficient b_2 is presented in Fig. 13, and the correlation is given in Eq. (16).

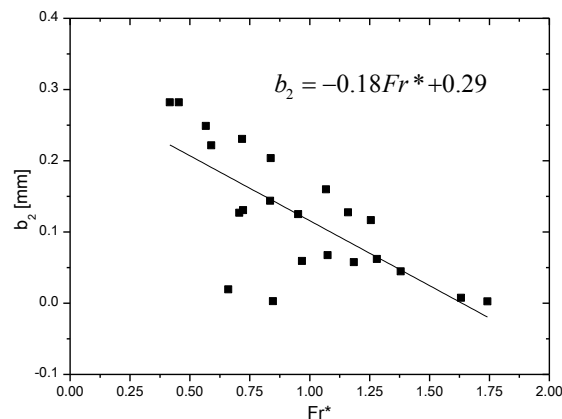


Figure 13. Coefficient b_2 as a function of the modified dimensionless Froude number.

$$b_2 = -0.18Fr^* + 0.29 \quad (16)$$

The coefficient w , which might be described as the spatial frequency of the Fourier function, is presented against the Froude number in Fig. 14, and the linear correlation is given in Eq. (17).

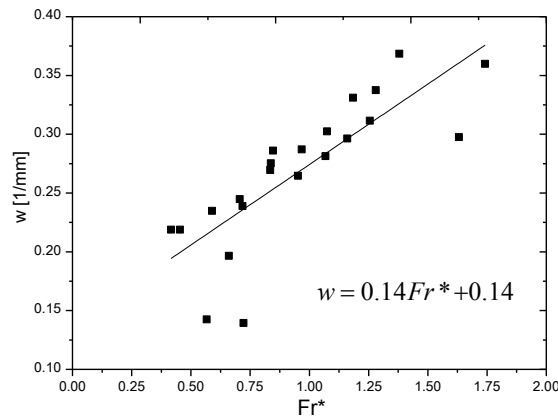


Figure 14. Coefficient w as a function of the modified dimensionless Froude number.

$$w = 0.14Fr^* + 0.14 \quad (17)$$

So, Eq. (11) might be rewritten as function of the dimensionless parameters of the flow, Eq. (18).

$$y_m = a_0(Fr^*) + a_1(Fr^*)\cos[w(Fr^*)x_m] + b_1(We^*)\sin[w(Fr^*)x_m] + a_2(We^*)\cos[2w(Fr^*)x_m] + b_2(Fr^*)\sin[2w(Fr^*)x_m] \quad (18)$$

With Eq. (18) and the modified Froude and Weber number it is possible to rebuild the interfacial wave of the wavy stratified water-heavy oil flows. This will be presented in the next section for several flow conditions.

6.2 Reconstruction of the interfacial wave

If the characteristics of the flow, of superficial velocities, fluid and pipe properties are known, Eqs. (12) - (17) can be used to calculate the coefficients of the Eq. (18), and so, the interfacial wave might be rebuilt. In this section a comparison between the mean interfacial waves given by the method proposed in the Section 4.2 and 5.2 and the one given by the generic equation.

Figures 15 to 17 present the mean wave and reconstructed for high water superficial velocities. In these cases the proposed method seems to be accurate in the reconstruction of the wavelength and wave amplitude of the interfacial wave, and the wave shape, resembling the sea wave, as said before.

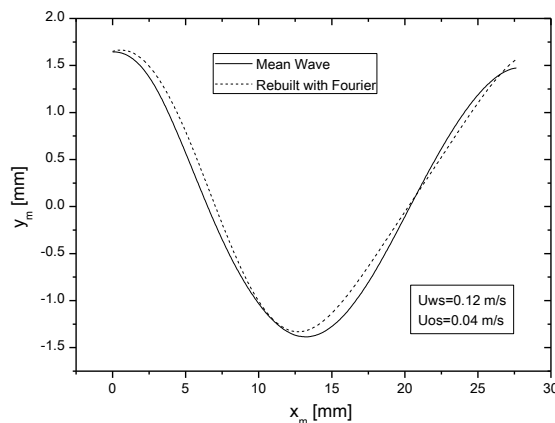


Figure 15. Comparison between mean wave and rebuilt by generic equation ($U_{ws}=0.12$ m/s and $U_{os}=0.04$ m/s)

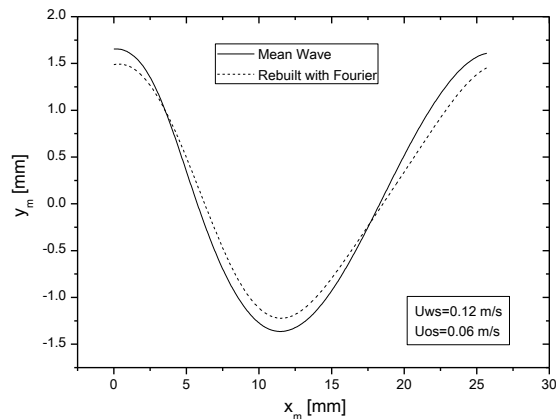


Figure 16. Comparison between mean wave and rebuilt by generic equation ($U_{ws}=0.12$ m/s and $U_{os}=0.06$ m/s)

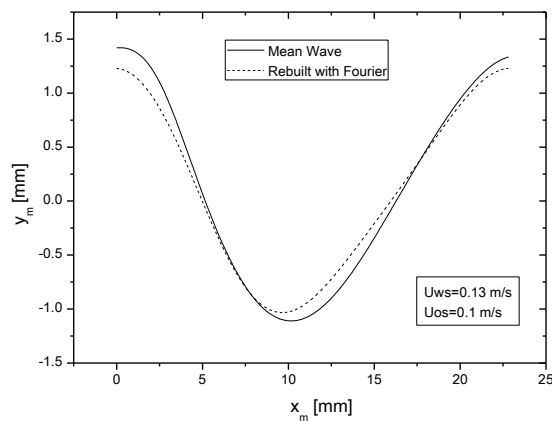


Figure 17. Comparison between mean wave and rebuilt by generic equation ($U_{ws}=0.13$ m/s and $U_{os}=0.1$ m/s)

Figures 18 and 19 present the reconstruction of waves for low water superficial velocities and high oil superficial velocities. In these cases, the method does not present good agreement with the prediction, by rebuilding a wave with bigger amplitude and smaller wavelength than the mean wave. This region represents a small slip between the phases, low relative velocity and low water holdup; these facts indicate low Weber numbers and high Froude numbers. It indicates that in these regions the dispersion of the points is so high that the proposed correlations for the coefficients of Eq. (18) are not suitable in marginal regions.

So, more experimental data are necessary, even in inclined flow, where the effect of gravity would be more prominent, and so, one can acquire more experimental points in the regions of low or high Froude and Weber numbers.

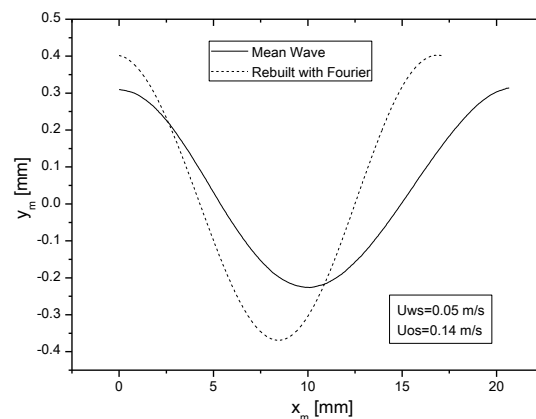


Figure 18. Comparison between mean wave and rebuilt by generic equation ($U_{ws}=0.05$ m/s and $U_{os}=0.14$ m/s).

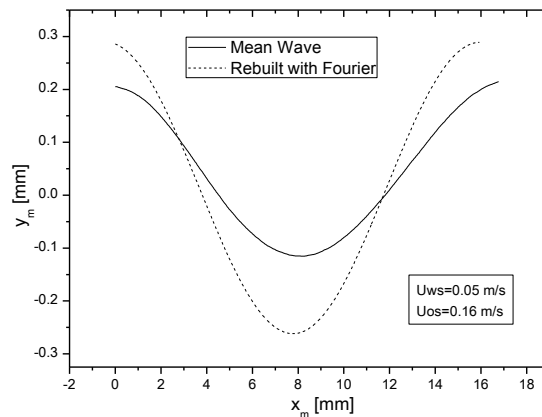


Figure 19. Comparison between mean wave and rebuilt by generic equation ($U_{ws}=0.05$ m/s and $U_{os}=0.16$ m/s).

7. CONCLUSIONS

The authors are proposing a generic equation to predict the characteristics of wavelength, amplitude and shape of the interfacial wave of water-heavy oil flows, and so, rebuild a mean wave.

The method uses a generic second order Fourier function where the coefficients are given as functions of dimensionless number of the flow; Weber and modified Froude numbers. These dimensionless numbers are functions of parameters of the flow as superficial velocities, and fluid and pipe properties.

Experimental data from literature were used to achieve the correlations for the coefficients of the generic equation.

The comparison in between experimental and reconstructed mean wave presents good agreement in the regions of medium Weber and Froude number; although this, in the regions of high Froude and low Weber numbers, where the relative velocity is small the equation predicts high differences between the experimental data and the rebuild wave. This could be explained by the high dispersion of the points in these regions, so the correlations proposed are not suitable for these areas.

So, more experimental data is needed to incorporate other factors, as gravitational forces, and so achieve more data in the regions where the correlations are not suitable.

8. ACKNOWLEDGEMENTS

The authors are grateful to FAPESP (Fundação de Amparo à Pesquisa do Estado de São Paulo, process 2010/03254-5) and PETROBRAS for the financial support.

9. REFERENCES

- Alkaya, B., Jayawarderna, S.S. and Brill, J.P., 2000. "Oil-water flow patterns in slightly inclined pipes". *Energy for the New Millennium*, Vol. 14, n. 17, p.1-8.
- Al-Wahaibi, T., Angeli, P., 2007. "Transition between stratified and non-stratified horizontal oil-water flows. Part I: Stability analysis", *Chemical Engineering and Science*, Vol. 62, p. 2915-2928.
- Al-Wahaibi, T., Smith, M. and Angeli, P., 2007. "Transition between stratified and non-stratified horizontal oil-water flows. Part II: Mechanism of drop formation". *Chemical Engineering and Science*, Vol. 62, p.2929-2940.
- Bannwart, A. C., Rodriguez, O. M. H., De Carvalho, C. H. M., Wang I. S. and Obregon Vara, R. M. 2004. "Flow Patterns in Heavy Crude Oil-water Flow". *Journal of Energy Resources Technology-Transactions of the ASME*, Vol. 126, p. 184-189.
- Bendat, J.S. and Piersol, A.G., 2000. *Random data: analysis and measurement procedures*. John Wiley & Sons, New York.
- Berthelsen, P.A. and Ytrehus, T., 2005. "Calculations of stratified wavy two-phase flow in pipes". *International Journal of Multiphase Flow*, Vol. 31, p. 571-592.
- Bontozoglou, V. and Hanratty, T.J., 1989. "Wave height estimation in stratified gas-liquid flows". *AiChE Journal*, Vol. 35, n. 8, p. 1346-1350.
- Bontozoglou, V., 1991. "Weakly nonlinear kelvin-helmholtz waves between fluids of finite depth". *International Journal of Multiphase Flow*, Vol. 17, n. 4, p.509-518.
- Brauner, N., Rovinsky, J. and Maron, D.M., 1996. "Determination of the interface curvature in stratified two-phase systems by energy considerations". *International Journal of Multiphase Flow*, Vol. 22, p. 1167-1185.

Marcelo S. de Castro and Oscar M. H. Rodriguez
 Interfacial Wave Shape Equation In Horizontal Wavy Stratified Water-Heavy Oil Flow

- Castro, M.S., Pereira, C.C., Santos, J.N. and Rodriguez, O.M.H., 2012. “Geometrical and kinematic properties of interfacial waves in stratified oil-water flow in inclined pipe”. *Experimental Thermal and Fluid Science*, Vol. 37, p.171-178.
- Castro, M.S. and Rodriguez, O.M.H., 2013. “Transition from wavy stratified flow to drops in horizontal heavy oil-water flow: a spatial phenomenon”. In *Proceedings of the International Conference on Multiphase Flow 2013 – ICMF 2013*. Jeju, Korea.
- Dyment, A. and Boudlal, A., 2004. “A theoretical model for gas-liquid slug flow in down inclined ducts”. *International Journal of Multiphase Flow*, Vol. 30, p. 512-550.
- Elseth, G., 2001. *An experimental study of oil-water flow in horizontal pipes*. Ph.D thesis. Norwegian University of Science and Technology, Porsgrunn, 270p.
- Li, G.J., Guo, L. and Chen, X.J., 1997. “An experimental investigation on the interfacial waves in air-water two-phase flow within horizontal pipelines”, *Chinese Journal of Chemical Engineering*, Vol. 5, p. 316-324.
- Ooms, G., 1972. “The hydrodynamic stability of core-annular flow of two ideal liquid”, *Applied Science Research*, doi:10.1007/bf01897844.
- Oliemans, R.V.A., 1986. *The lubricating-film model for core-annular flow*, Ph.D. Thesis, Technische Hogeschool Delft. Delft University, Delft, Netherlands.
- Ooms, G., Seagal, A., Van Der Wees, A.J., Meerhoff, R. and Oliemans, R.V.A., 1984. “A theoretical model for core annular flow of a very viscous oil core and a water annulus through a horizontal pipe”. *International Journal of Multiphase Flow*, Vol. 10, p. 41–60.
- Feng, J., Huang, P.Y. and Joseph, D.D., 1995. “Dynamic simulation of the motion of capsules in pipelines”, *Journal of Fluid Mechanics*, Vol. 286, p. 201–27.
- Pereira, C.C., 2011. “Estudo experimental e modelagem do escoamento estratificado ondulado óleo-água”. *Dissertation*, University of São Paulo, São Paulo, Brazil.
- Rodriguez, I.H., Yamaguti, H.K.B., Castro, M.S., Da Silva, M.J. and Rodriguez, O.M.H., 2011. “Slip ratio in dispersed viscous oil–water pipe flow”. *Experimental Thermal and Fluid Science*, Vol. 35, n. 1, p. 11-19.
- Trallero, J. L., 1995. *Oil-Water Flow Patterns in Horizontal Pipes*. PhD thesis, The University of Tulsa, Tulsa, Oklahoma, USA.
- Trallero, J.L., Sarica, C. and Brill, J.P., 1997. “A study of oil/water flow patterns in horizontal pipes”. *SPE Production and Facilities*, Vol. 12, n.3, p.165-172.
- Wallis, G.B., 1969. *One-dimensional two-phase flow*. MacGraw-Hill, New York, 408p.
- Wang, Z.L. Gabriel, K.S. and Manz, D.L., 2004a. “The Influences of wave height on the interfacial friction in annular gas-liquid flow under normal and microgravity conditions”, *International Journal of Multiphase Flow*, Vol. 30, p. 1193-1211.
- Wang, Z.L. Gabriel, K.S. and Zhu, Z.F., 2004b. “The effects of gravity on the features of the interfacial waves in annular two-phase flow”, *Microgravity Science and Technology*, Vol. 15, p. 19-27.

10. RESPONSIBILITY NOTICE

The authors are the only responsible for the printed material included in this paper.